

# Direct-Indirect Hybrid Implosion in Heavy Ion Inertial Fusion

Yoshifumi IIZUKA<sup>1</sup>, Shigeo KAWATA<sup>1</sup>, Tomohiro KODERA<sup>1</sup>, Alexander I. OGOYSKI<sup>2</sup>  
and Takashi KIKUCHI<sup>1</sup>

<sup>1</sup>*Utsunomiya University, Utsunomiya, Tochigi 321-8585, Japan*

<sup>2</sup>*Technical University of Varna, Varna 9010, Bulgaria*

(Received: 31 July 2008 / Accepted: 12 November 2008)

The key issues in heavy ion beam (HIB) inertial confinement fusion include particle accelerator, physics of intense beam, beam final transport, target-plasma hydrodynamics, and so on. In this paper, we focus on a fuel implosion. In order to realize an effective implosion, beam illumination non-uniformity on a fuel target must be suppressed less than a few %. In this study a direct-indirect hybrid implosion mode is discussed in heavy ion beam inertial confinement fusion (HIF) in order to release sufficient fusion energy in a robust manner. In the direct-indirect hybrid mode target, a low density foam layer is inserted, and the radiation energy is confined in the foam layer. In the foam layer the radiation transport is expected to smooth the HIB illumination non-uniformity in the lateral direction. In this paper, we study the influences of the foam thickness and the inner radiation-shield Al density on the implosion uniformity. Two-dimensional fluid simulations demonstrate that the hybrid target contributes to the HIB non-uniformity smoothing and releases a sufficient fusion energy output in HIF.

**Keywords:** Inertial confinement fusion, Heavy ion beam, Direct-indirect hybrid implosion

## 1. Introduction

The important issues in heavy ion beam (HIB) inertial confinement fusion (ICF) include non-uniformity of driver-beam illumination to a fuel pellet in a reactor [1-8]. The HIB illumination non-uniformity induces the implosion non-uniformity. As a result, output fusion energy may be reduced. Therefore, the driver-beam illumination non-uniformity must be suppressed less than a few percent in order to achieve a symmetric fuel pellet implosion in the ICF [8-11]. In our study, in order to study the non-uniformity smoothing effect by the radiation transport effect on the pellet implosion, the hydrodynamic code is coupled with the HIB illumination code [12]. Simulation results in this paper demonstrate that the radiation energy confined smoothes the HIB illumination [13-14]. In our simulations, we employ a foam layer to increase the radiation energy confined at the low density foam region. We call this target a direct-indirect hybrid target in this paper.

## 2. Simulation Model

In HIF, the pulse HIBs irradiate a fuel target. During the HIB illumination, the fuel target becomes a plasma. Therefore the behavior of the target can be treated as a plasma fluid. In our study, the physical model employed is based on a three-temperature (an ion, an electron and a radiation temperature) fluid model. We also employ a heat conduction and a radiation transport. In our 2-dimentional hydrodynamic code developed, we solve basic hydrodynamic equations. In our simulation code the ALE method [15-17] is employed, and the meshes move only in the radial direction. In calculations of the implosion, the equation of state is evaluated by using a fitting formula of

the SESAME Library [18] based on the Thomas-Fermi model.

The hybrid target pellet employed in this study is shown in Fig. 1 (a). In Fig. 1 (a) the target consists of five layers of a solid Pb, a solid Al, a foam Al, a solid Al and DT. The external radius is 4.0mm, the outer Pb layer thickness is 30  $\mu\text{m}$ , the outer Al layer thickness is 470  $\mu\text{m}$  and the inner Al thickness is 73  $\mu\text{m}$ . The Pb mass density is 11.3  $\text{g}/\text{cm}^3$ . The Al mass density is 2.69  $\text{g}/\text{cm}^3$ . The mass density of the foam layer is 0.01% of the Al solid density. The DT mass is 2.55mg. In our study we employ  $\text{Pb}^+$  ion HIBs with the mean particle energy of 8GeV. We employ the 32-HIBs illumination system [19-21]. The total energy is 4.0MJ. The beam particle density distribution is in the Gaussian. The longitudinal temperature of HIB ions is 100 MeV with the Maxwell distribution. The HIB pulse consists of a foot pulse and a main pulse as shown in Fig. 1 (b). The target and HIB parameter are selected so that all the HIB particles deposit their energy at the outer Al layer.

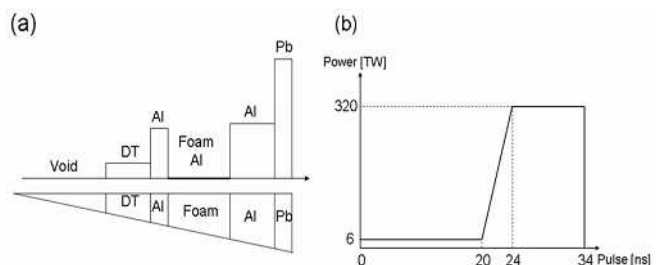


Fig. 1. (a) Fuel target structure. (b) The HIB pulse consists of a foot pulse and a main pulse.

In this section, we employ the 32-HIBs illumination system [19-21]. To see the radiation transport effect on the implosion non-uniformity smoothing, we compare the results for the case with the radiation transport (ON) and without the radiation transport (OFF) for the target shown in Fig.1 (a). Figure 2 presents the time dependence of the RMS non-uniformity of the radiation temperature at the ablation front in the case of the radiation transport ON and OFF. In Fig.2 we see that the implosion non-uniformity at the ablation front becomes small effectively by the main pulse in the case of the radiation transport ON. During the main pulse, the implosion non-uniformity can be smoothed by the radiation transport effect.

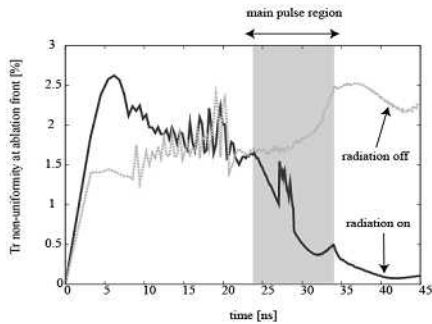


Fig. 2. The histories of the RMS non-uniformity of the radiation temperature at the ablation front in the case of the radiation transport ON and OFF.

Figure 3 presents the time dependence of the confined radiation energy at the low density region. The peak conversion efficiencies of the HIB total energy on the radiation energy are  $\sim 4.5\%$  in the case of the 0.5mm foam and  $\sim 1.5\%$  in the case without the foam. From these results, we find that the implosion mode in the case with the foam may be a hybrid of direct driven and indirect driven modes.

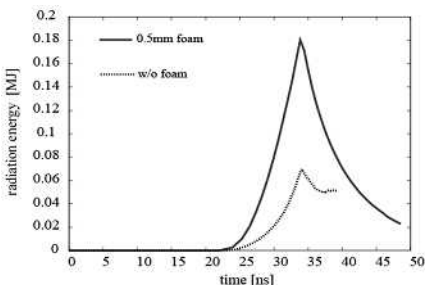


Fig. 3. Time dependence of the confined radiation energy at the low density region in the case of 0.5mm foam and in the case of without the foam.

### 3. Effect of foam thickness

In the foam layer the radiation is expected to smooth the HIB illumination non-uniformity in the lateral direction. In this section, we use the direct-indirect hybrid target (see Fig. 1 (a)). In order to study the influence of the foam

thickness on the implosion, the foam thickness is changed between 0.6mm to 1.0mm. The Al foam density is 0.01% of the solid density. When we change the foam thickness, the foam outer radius is fixed and the inner radius is changed; the DT fuel mass is fixed. Figure 4 shows the gain versus the foam thickness. The required fusion gain is about 30 for HIB ICF (HIF). Figure 4 presents that there is the optimum foam thickness.

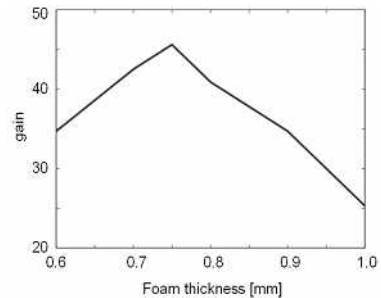


Fig. 4. Pellet gain versus the foam thickness

Figure 5 (a) shows the radiation temperature non-uniformity and the ion temperature non-uniformity in the Al layer versus the foam thickness at the void closure time. Figure 5 (b) shows the implosion efficiency versus the foam thickness. We define the implosion efficiency as follows:  $E_{DTK}/E_{total}$   $E_{DTK} = 1/2 m_{DT} v^2_{DT}$ . Here,  $E_{total}$  is the input total beam energy. Figures 5 (a) and (b) show that the implosion non-uniformity and the implosion efficiency decrease with the increase in the foam thickness.

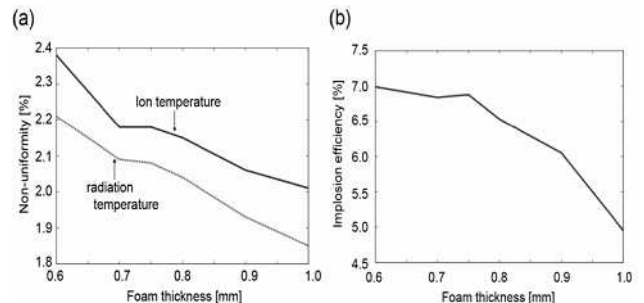


Fig. 5. Foam thickness versus (a) non-uniformities and versus (b) the implosion efficiency at the void closure time.

Figure 6 shows the comparison of pressure profiles for the case of the 0.6mm foam (34ns) and the 1.0mm foam (37ns) at the time, at which the main shock wave reaches the outer surface of the DT layer. In the case of 0.6mm foam thickness, the implosion velocity at the void closure time is  $3.1 \times 10^5 \text{ m/s}$ . In the case of 1.0mm foam thickness, the implosion velocity is  $2.5 \times 10^5 \text{ m/s}$ . When the foam thickness becomes too thick, the implosion velocity decreases and a sufficient implosion pressure can not be obtained. Therefore, the pellet gain becomes small in the case of the thick foam. The results indicate that the foam

thickness is important parameter to obtain a sufficient fusion energy output.

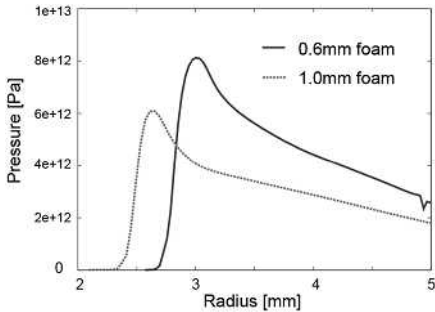


Fig. 6. Pressure profiles for the case of the 0.6mm foam (34ns) and the 1.0mm foam (37ns).

#### 4. Effect of inner Al density

This section presents the effect of the inner Al density on the hybrid target implosion. In order to obtain a sufficient high gain when the foam thickness becomes thick, we need to keep the implosion efficiency high. In this section, we focus on the inner Al layer (see Fig. 1 (a)) to improve the implosion efficiency for a target, which has the thick foam. The inner Al has the roles of the DT fuel pusher and the prevention of the fuel pre-heating. We employ the inner Al density, which can shield the radiation. In order to study the inner Al density influence on the implosion, the inner Al density varies in four cases. The inner Al density varies among  $2.69 \text{ g/cm}^3$  ( $\rho = \rho_s$  (solid density)), 10% of the Al solid density ( $\rho = \rho_s / 10$ ), 1% of the Al solid density ( $\rho = \rho_s / 100$ ) and 0.1% of the Al solid density ( $\rho = \rho_s / 1000$ ). The target external radius is 4.0mm, the outer Pb layer thickness is  $30 \mu\text{m}$ , the outer Al layer thickness is  $470 \mu\text{m}$  and the inner Al thickness is  $73 \mu\text{m}$ . The Pb mass density is  $11.3 \text{ g/cm}^3$ . The Al mass density is  $2.69 \text{ g/cm}^3$ . The mass density of the foam layer is 0.01% of the Al solid density. The DT mass is 2.55mg. We also employ the 32-HIBs illumination system [19 -21].

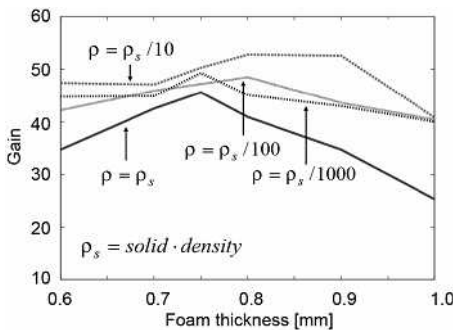


Fig. 7. Pellet gain versus the foam thickness for the various inner Al densities.

Figure 7 shows the gain versus the foam thickness for the various inner Al densities  $\rho$ . Figure 7 shows that there is the optimum density for the inner Al layer. In the case of  $\rho = \rho_s / 10$  a high gain is obtained and the target is robust against the change in the foam Al thickness. The implosion velocity in the case of  $\rho = \rho_s / 1000$  at void closure time is  $3.1 \times 10^5 \text{ m/s}$  in the case of 0.6mm foam thickness and is  $3.0 \times 10^5 \text{ m/s}$  in the case of 1.0mm foam thickness. Figures 8 show the non-uniformities in the Al layer versus the foam thickness at the void closure time: (a) the pressure non-uniformity, (b) the density non-uniformity. The inner Al density has influence on the implosion non-uniformity. When the inner Al density becomes lower, the implosion non-uniformity decreases. The low density inner Al behaves as a cushion or a buffer to mitigate the non-uniformity. In addition, the effective thickness of the Al foam layer becomes large, when the inner Al layer density becomes lower. As shown in Fig. 5 (a), the thicker the foam layer becomes, the lower the non-uniformity becomes.

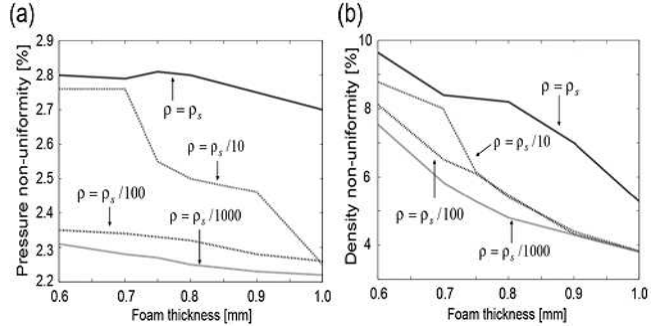


Fig. 8. Foam thickness versus non-uniformities in the Al layer at void closure time: (a) pressure non-uniformity and (b) density non-uniformity for the various inner Al densities.

Figure 9 shows the isentrope parameter  $\alpha$  at the void closure time:  $\alpha = p(\rho_{DT}, T) / p_{deg}(\rho_{DT})$ , where  $p_{deg}(\rho_{DT}) = A_{deg} \rho_{DT}^{5/3}$ ,  $\rho_{DT}$  is the average DT density and  $A_{deg} = 2.17 \times 10^{12} (\text{erg/g}) / (\text{g/cm}^3)^{2/3}$ . In ICF,  $\alpha$  should be kept small as possible [22]. In Fig. 9, when the inner Al density is kept high, ( $\rho = \rho_s$  or  $\rho = \rho_s / 10$ ),  $\alpha$  is kept small successfully. However, when the inner Al density becomes lower ( $\rho = \rho_s / 100$  or  $\rho = \rho_s / 1000$ ), the pre-heating effect becomes significant (see Fig. 9). We think that it is possible to shield it at  $\rho = \rho_s / 10$  and high gain is obtained in the case of  $\rho = \rho_s / 10$  as shown in Fig. 7. These results indicate that the inner Al density is an important parameter to obtain a sufficient fusion energy output.

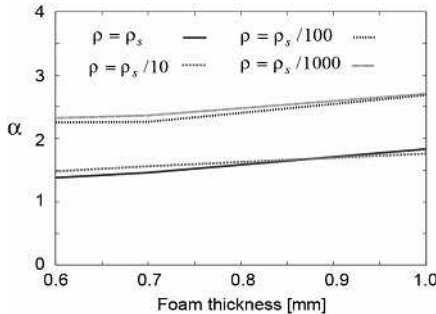


Fig. 9. Isentrope parameter versus the foam thickness for the various inner Al densities.

## 5. Conclusions

In this paper, we discussed the target implosion non-uniformity smoothing in a direct-indirect hybrid target by using a low density foam layer. The direct driven fuel target implosion was weak against the beam non-uniformity. However, in the low density foam region, the radiation energy is confined and then the implosion non-uniformity is smoothed. Therefore, we employ the foam layer for the fuel target in order to realize a uniform implosion. We studied the influences of the foam thickness and the inner Al density on the implosion in the direct-indirect hybrid target. From our calculation results, the change in the foam thickness has an influence on the implosion. When the foam thickness becomes thick, the implosion non-uniformity decreases. However, the implosion efficiency is not sufficient for the thick foam. Therefore there is the optimum foam thickness on the implosion. The foam thickness is the important parameter to release the sufficient fusion energy. We also study the effect of the inner Al density on the implosion. In our calculation results, when the inner Al density becomes lower, the implosion velocity can be kept high, and the implosion non-uniformity decreases. However, if the inner Al density is too low, the fuel pre-heating cannot be prevented. Therefore, the inner Al density is the important parameter to obtain a sufficient fusion energy output. Our results present that in HIF the direct-indirect hybrid implosion mode is realized by employing the foam layer in the spherical target.

## 6. Acknowledgments

This work was partly supported by the JSPS (Japan Society for the Promotion of Science) and MEXT (Ministry of Education, Culture, Sports, Science and Technology). We would also like to present our thanks to colleagues in the Japan and US HIF VNL research group for their fruitful discussions on this subject. This work is also supported by CORE (center for Optical Research and Education) in Utsunomiya University.

## 7. References

- [1] J. D. Lindl, R. W. Mcrory, and M. Campbell, Phys. Today **45**, 32 (1992).
- [2] W. J. Hogan, R. Bangerter, and GL. Kulcinski, Phys. Today **45**, 42 (1992).
- [3] M. Tabak and D. Callahan-Miller, Phys. Plasmas **5**, 1895 (1998).
- [4] M. Tabak and D. Callahan-Miller, Nucl. Instrum. Methods in Phys. Res A. **415**, 7(1998).
- [5] D. A. Callahan, Appl. Phys. Lett. **67**, L3254 (1995).
- [6] T. Someya, S. Kawata, T. Nakamura, A. I. Ogoyski, K. Shimizu, and J. Sasaki, Fusion Science and Tech. **43**, 282 (2003).
- [7] W. M. Sharp, D. A. Callahan, M. Tabak, S. S. Yu, et al., Fusion Science and Tech. **43**, 393 (2003).
- [8] J. Sasaki, T. Nakamura, Y. Uchida, T. Someya, et al., Jpn. J. Appl. Phys. **40**, L968 (2001).
- [9] M. Murakami, Appl. Phys. Lett. **27**, 1587 (1995).
- [10] S. Skupsky, K. Lee, J. Appl. Phys. **54**, 3662 (1983).
- [11] S. Kawata and K. Niu, J. Phys. Soc. Jpn. **53**, 3416 (1984).
- [12] A. I. Ogoyski, T. Someya and S. Kawata, Camp. Phys. Comm. **157**, 160 (2004).
- [13] T. Someya, K. Miyazawa, T. Kikuchi, S. Kawata, Laser Part. Beam **24**, 359-369 (2006).
- [14] G. O. Allshouse, R. E. Olson, D. A. Callahan-Miller, M. Tabak, Nuc. Fus. **39**, 893 (1999)
- [15] C. W. Hirt, A. A. Amsden and J. L. Cook, J. Comp. Phys. **135** 203 (1997).
- [16] M. Kucharik, J. Limpouch, R. Liska and P. Vachal, Czech. J. Phys. **54** 391 (2004).
- [17] A. L. Nichols, R. Couch, J. D. Maltby, R. C. McCallen, I. Otero and R. Sharp, UCRL-JC-124706 (1996).
- [18] A. R. Bell, Rutherford Lab. Report, RL-80-091 (1981).
- [19] T. Someya, S. Kawata, T. Kikuchi, A. I. Ogoyski, Nucl. Instrum. Methods, Phys. Res. A **544**, 406 (2005).
- [20] A. I. Ogoyski, T. Someya, T. Sasaki, S. Kawata, Phys. Lett. A **315**, 372 (2003).
- [21] T. Someya, A. I. Ogoyski, S. Kawata, T. Sasaki, Phys. Rev. ST Accel. Beam **7**, 04470 (2004).
- [22] S. Atzeni, J. Meyer-ter-vehn, *the physics of inertial fusion* (Clarendon Press, Oxford, 2004), p. 52.